

Effects of bovine milk osteopontin on in vitro enamel remineralization as a topical application prior to immersion in remineralizing solutions with/without fluoride.

Hisako Ishizuka

Tokyo Dental College

Hidenori Hamba

Tokyo Dental College

Keiki Nakamura

Tokyo Dental College

Yoshihito Miyayoshi

Tokyo Dental College

Haruto Kumura

Hokkaido University

Takashi Muramatsu (✉ tmuramat@tdc.ac.jp)

Tokyo Dental College

Research Article

Keywords: Bovine milk osteopontin, Remineralization, Micro-CT, Fluoride

Posted Date: April 22nd, 2022

DOI: <https://doi.org/10.21203/rs.3.rs-1552030/v1>

License:  This work is licensed under a Creative Commons Attribution 4.0 International License.

[Read Full License](#)

Abstract

Objectives The aim of the present study was to investigate the effects of bovine milk osteopontin (OPN) on enamel remineralization as a topical application.

Materials and methods After bovine enamel blocks were immersed in demineralizing solution, they were divided into the following 3 groups: OPN (2.7 and 5.4 μM) solutions and deionized water (negative control), which were applied to the enamel surface of each specimen at 37°C for 30 min. Each group was divided into 2 groups and immersed in remineralizing solution with or without 1 ppm of fluoride (F). After demineralization and remineralization, specimens were scanned by micro-computed tomography to evaluate mineral density and calculate mineral loss. At 14 days, surface and cross-sectional images were observed under a scanning electron microscope (SEM).

Results Remineralization was confirmed in all groups. The percentage of remineralization was higher in remineralization solution with than without F ($p < 0.05$). OPN groups in remineralizing solution without F showed a lower percentage of remineralization at 14 days. In the presence of F, the percentage of remineralization was similar in the 5.4 μM OPN group and control group and significantly lower in the 2.7 μM OPN group ($p < 0.05$). SEM images showed the accumulation of crystal-like deposits on the enamel surface in the OPN groups, and needle-like structural precipitations were observed in the OPN with F groups. Furthermore, stable structures were detected at the subsurface region.

Conclusions These results suggest that bovine milk OPN inhibits remineralization in solution without F, but 5.4 μM bovine milk OPN does not inhibit remineralization using solution containing F.

Clinical relevance Application of 5.4 μM bovine milk OPN prior to immersion in solution with F would be a potential for the management of dental caries in the future, from a viewpoint of both bacteria and remineralization.

Introduction

Demineralization and remineralization occur on the enamel surface, and the balance between these processes is maintained under an oral environment. A disruption in this balance eventually leads to the development of dental caries [1–3]. White-spot lesions in the early stage of the dental caries process prior to cavitation are a representative clinical finding that is histologically observed in the mineral-poor region of the enamel subsurface with an intact surface layer [4]. The remineralization of enamel, a natural repair process, occurs at the demineralized region, with plaque/salivary calcium (Ca^{2+}) and phosphate (PO_4^{3-}) ions being deposited in crystal voids, which results in mineral gain. The presence of free fluoride (F^-) ions in the oral environment increases the incorporation of Ca^{2+} and PO_4^{3-} ions into the crystal lattice [5]. Therefore, an effective method for dental caries management is to improve the remineralizing process using remineralization products [6, 7]. New improved biochemical materials need to possess properties that achieve enamel remineralization even in saliva with low Ca^{2+} and PO_4^{3-} ions concentrations [8].

These materials include bioactive glass (BAG) [9], casein phosphopeptide-amorphous calcium phosphate (CPP-ACP) [10], and functionalized β -tricalcium phosphate (fTCP) [11]. Surface biomineralization is another new approach to improve remineralization with advances in peptide design [12]. These materials ideally need to be naturally derived and consist of similar components to saliva.

Osteopontin (OPN), a non-collagenous protein, was initially detected in bone, but is also present in teeth, soft tissues, and physiological fluids including the kidneys and mammary and salivary glands [13–19]. OPN has also been detected in saliva and bovine milk [20]. Milk OPN has multiple functions in early and adult life [21]. A high concentration of OPN is present in human milk [22–24], and commercial infant formulas with OPN have recently become available. Previous studies showed that bovine milk OPN bound directly to bacteria and enhanced phagocytosis [25], and also prevented oral bacterial adhesion to the tooth surface and reduced oral biofilm formation and pH drops [26–28]. OPN is a phosphorylated glycoprotein, and Kumura et al. [29] reported the inhibitory effects of bovine milk OPN and its fragments on the formation of calcium phosphate precipitates. However, the effects of bovine milk OPN on enamel remineralization currently remain unknown.

Topical application of protein essentially inhibits uptake of mineral to enamel. Earlier reports showed that combination of casein and 1 ppm F increase quantity of mineral uptake [30, 31]. We therefore hypothesize the application of OPN to a tooth surface inhibits to intake the mineral, but F in remineralization solution recovers to intake the mineral. In the present study, we investigated the effects of bovine milk OPN, as a potential caries preventive agent in saliva, on the remineralization of enamel lesions using remineralizing solutions with or without fluoride *in vitro*.

Materials And Methods

Ethics approval

The study was performed using food industry animal carcass waste, and ethical approval was not required for waste tissues. The bovine teeth used in this study were stored and disposed under the direction of the guidelines and policies of Tokyo Dental College (reference number: 2020-103-02).

Specimen preparation

Thirty bovine incisors were purchased from Yokohama Meat Corporation (Yokohama, Japan), and were cryopreserved and defrosted using running tap water immediately before use. After the surrounding periodontal tissues had been mechanically removed, the coronal pulp tissues and roots were also removed. The crowns of teeth were cut into 3×3×2 mm pieces, and enamel-dentin blocks were prepared using a low-speed diamond saw (Isomet, Buehler, Lake Bluff, IL, USA) under water-cooling conditions. These blocks were embedded into epoxy resin (EpoxiCure 2, Buehler, Lake Bluff, IL, USA), and their enamel surfaces were flatly ground with 600- to 2000-grit silicon carbide (SiC) papers (Fuji Star, Sankyo Rikagaku, Saitama, Japan) under running water. The edge (1 mm) of the surface was coated by applying nail varnish (Revlon Red 680; Revlon, New York, NY, USA) and an observation window (2×2 mm) was

created by exposing the polished enamel surface of each specimen. A hole (1 mm in diameter and 0.5 mm in depth) was formed at the side of each specimen using a diamond bur (440SS ISO # 010, Shofu, Kyoto, Japan) as a reference point for micro-computed tomography (micro-CT) scans.

The specimens were randomly allocated into 6 groups (n = 9 each) based on the concentration of OPN (0 μ M, 2.7 μ M and 5.4 μ M) and F (0 or 1ppm) in remineralization solution as described below.

Demineralization

Each specimen was put in a 2mL-microtube and immersed in 2 mL of demineralizing solution (17.8 mM CaCl₂, 8.8 mM KH₂PO₄, and 100 mM lactic acid; the pH of the solution was adjusted to 4.3 with 10 mM KOH) at room temperature for 6 to 8 days according to the method by Margolis et al. [32] with modifications. Demineralizing solution was refreshed daily.

We checked all the demineralized specimens by use of micro-CT scan and analysis software Ratoc as described below. The specimens that had extreme deep or shallow demineralization in depth were excluded.

Application of bovine milk OPN

OPN derived from bovine milk was purchased from Sigma-Aldrich (St. Louis, MO, USA). OPN was dissolved in deionized water without precipitation. The concentration of OPN was determined in reference to Schlafer et al. [26]. After demineralization, 10 μ L of OPN (final concentrations of 2.7 and 5.4 μ M) was applied to the enamel surface of each specimen at 37°C for 30 min. Specimens were then rinsed off using deionized water for 10 seconds. As a negative control, deionized water was applied instead of OPN.

Remineralization

Remineralizing solution (1.5 mM CaCl₂-2H₂O, 0.9 mM KH₂PO₄, 130 mM KCl, 20 mM HEPES, and NaF 1mg/L; pH adjusted to 7.0 with 10 mM KOH) was prepared according to the method by ten Cate & Duijsters [33]. Remineralizing solution containing F⁻ (1ppm) was also used in the present study according to the method by Romero *et al.* [30]. Each specimen was separately put in the 2mL-microtube and immersed in 2mL of remineralizing solution at 37°C for 14 days. The remineralizing solution was changed every day. At 7 and 14 days, specimens were scanned by micro-CT and observed under a scanning electron microscope (SEM) at 14 days (Fig. 1).

Micro-CT scanning and image analysis

After demineralization and remineralization, a micro-CT system (InspeXio SMX-100CT, Shimadzu, Kyoto, Japan) was used to evaluate the mineral density (MD) of specimens. The micro-CT system generates polychromatic X-rays with cone-beam geometry. A 0.2-mm-thick brass plate was set in the beam path to reduce the beam-hardening effect. The tube voltage was 100 kV at a current of 100 μ A. The specimen was mounted on a turntable to vertically irradiate X-rays on the enamel surface. A series of mineral reference phantoms were also scanned for MD calibration and included three hydroxyapatite (HAp) disks

(TRI/3D-BON, Ratoc, Tokyo, Japan); two with different concentrations (0.50 and 0.70 gHAp/cm³) of HAp crystals mixed with epoxy resin (Epoxicure Resin, Buehler) and one pure HAp disk (3.16 gHAp/cm³) (Cellyard, Hoya, Tokyo, Japan). The phantoms were scanned in a plastic tube, which was almost the same as the imaging conditions of the specimens.

Scanned data were reconstructed from 2-dimensional (2D) images with a resolution of 512 × 512 pixels to a 3-dimensional (3D) image using 3D analysis software (TRI/3D-BON, Ratoc). These images were used for visualization and quantitative volumetric measurements. CT values were converted into MD values (gHAp/cm³) using a linear calibration curve based on the grey values obtained from the mineral reference phantoms. The MD profile of each specimen was obtained by plotting MD (vol%). Maximum MD in each specimen was normalized to 100 vol% against depth. To minimize ring artifacts, air calibration of the detector was carried out prior to each scanning, and 6-frame averaging was also applied in the acquisition phase to improve the signal-to-noise ratio (SNR) [34]. For correction of beam hardening, a 0.2-mm thick brass (Cu–Zn) filter was installed in the beam path to reduce beam-hardening effect [35].

The percentage of remineralization was calculated according to standard procedures [36]. Lesion depth (LD) was set at the depth from the original enamel surface (covered area with varnish), and mineral loss (ΔZ) (vol% μm) was integrated mineral loss up to the lesion depth. To evaluate the extent of repair, the relative change in percentage of remineralization (%R) was calculated as follows: $\%R = (\Delta Z \text{ in DEM} - \Delta Z \text{ in REM}) / \Delta Z \text{ in DEM} \times 100$.

SEM observations

Specimens were prepared in the same manner as described for micro-CT observations. The enamel surface at the treatment window was observed under a field emission SEM (SU6600, Hitachi High Technologies, Tokyo, Japan) at ×3500 magnification, following a specimen processing protocol for SEM, which included desiccation and carbon sputter coating. After observation of enamel surface, the specimen was cut with diamond pointed burs and nippers, and cross-sectioned surface was observed under SEM. Cross-sections were also observed at the same magnification.

Statistical analysis

The results of percentage of remineralization (%R) were expressed as the mean and standard deviation. Differences within and between the mean values of groups were statistically analyzed using a two-way repeated-measures analysis of variance (ANOVA) with application and period as factors and Tukey's test. The significance level of all tests was set at $\alpha = 0.05$.

Results

Micro-CT analysis

An X-ray transmission image of the specimen immersed in demineralizing solution for 6 to 8 days showed demineralization on the surface layer of enamel (Fig. 2, left column). In all groups, radiopacity

was observed in the demineralized lesions after 7 and 14 days. Radiopacity became noticeable at 14 days in specimens in solution with fluoride (the F (+) group) compared to that without F (the F (-) group).

Percentage of remineralization

Table 1 shows the mean percentage of remineralization of all groups.

In all groups, the percentage of remineralization was higher after 14 days than after 7 days. The percentage of remineralization was higher in the F (+) group than in the F (-) group ($p > 0.05$) (Table 1).

In the F (-) group after 7 days, no significant difference was observed in the percentage of remineralization among the three groups (Table 1). After 14 days, the percentage of remineralization was significantly higher in the control group than in the OPN 2.7 μM and OPN 5.4 μM groups ($p < 0.05$) (Table 1). No significant differences were observed between the OPN 2.7 μM and OPN 5.4 μM groups.

In the F (+) group after 7 days, the percentage of remineralization was significantly lower in the OPN 2.7 μM group than in the control group after immersion in remineralizing solution ($p < 0.05$), and no significant differences were observed between the control and OPN 5.4 μM groups. After 14 days, the percentage of remineralization was significantly lower in the OPN 2.7 μM group than in the control and OPN 5.4 μM groups. ($p < 0.05$), and no significant differences were observed between the control and OPN 5.4 μM groups.

SEM observations

After 14 days, compared to the groups of demineralization (Fig. 3a) and control without F (Fig. 3b), a crystal-like deposit of approximately 1 μm in size was observed in OPN (+) of the F (-) groups (Figs. 3c and 3d). At OPN 5.4 μM , more deposits were detected on the enamel surface than at OPN 2.7 μM (Figs. 3c and 3d). Needle-like deposits were observed in the F (+) group (Figs. 3e, 3f and 3g).

In cross-sectional images, a sparse structure was confirmed at the subsurface region after demineralization (Fig. 4a). In the F (-) group after 14 days, the sparse structure disappeared in the control group (Fig. 4b), but remained in the OPN (+) groups (Figs. 4c and 4d). In the F (+) group, the sparse structure disappeared compared with the F (-) groups (Figs. 4e, 4f and 4g). At the surface, needle-like precipitation structures were seen on the surface in OPN 5.4 μM -F(+) group (Fig. 4g), while they were not observed in other groups (Figs. 4b-4f).

Discussion

The present results demonstrated that remineralization of demineralized bovine enamel occurred even in the presence of bovine milk OPN.

In this study, we used bovine enamel. Human enamels have many individual differences including age and composition by daily brushing or topical application of F, and would result in variability of the results.

Furthermore, we need enough flat smooth surfaces for specimens, and human enamels are insufficient. Concern points of the bovine enamel include that crystal size is bigger than human enamel, but we did not focus on the change of the crystal size and structure in this study. Therefore, we used bovine enamel in this study.

Salivary phosphoproteins, such as acidic proline-rich proteins (PRPs) and statherins, stabilize high concentration of Ca^{2+} and PO_4^{3-} to facilitate ion bioavailability for mineralization. They inhibit phase change in solution, but upon interaction with the tooth surface bound ions can be made bioavailable. Advantages of introducing phosphoprotein to simulate the mineral-stabilizing properties of saliva have been proposed [30]. Saliva and bovine milk contain phosphorylated OPN [24, 29, 37–39], and, thus, the application of OPN to the enamel surface may be made bioavailable. However, the effect has been unknown. Our micro-CT images showed radiopacity became noticeable at the demineralized areas despite OPN application at 7 and 14 days, and the percentage of remineralization (%R) at 14 days was higher than that at 7 days in corresponding group. The results suggest percentage of remineralization in demineralized enamel gains despite the application of bovine milk OPN. This is the first study to examine the effects of bovine milk OPN on enamel remineralization. However, the degree of mineralization was affected by fluoride added to artificial saliva; the percentage of remineralization was higher in F (+) solution than in F (-) solution.

In F (-) solution, the percentage of remineralization was significantly higher in the control group than in the OPN groups at 14 days, suggesting that OPN inhibited remineralization. The SEM analysis showed the accumulation of crystal-like deposits on the surface of enamel in the 2.7 μM and 5.4 μM groups. The enamel surface is covered by salivary proteins and molecules, such as statherin and PRPs, which are important constituents of acquired pellicles [4]. OPN has Ca^{2+} -binding sites [40] and binds to HAp on the enamel surface. Therefore, milk bovine OPN binds not only to HAp on the enamel surface, but also to Ca^{2+} in remineralization solution. As a result, the entrance of Ca^{2+} into the subsurface area was blocked at the enamel surface in F (-) solution.

The percentage of remineralization was higher in F (+) solution than in F (-) solution. At 14 days. SEM images showed a firm structure at the subsurface region and needle-like structural precipitations, which may be composed of F and F-related minerals, such as CaF_2 , because they were not observed in remineralization solution without F. In previous experimental studies using salivary macromolecules with F in artificial saliva, they were adsorbed on the enamel or dentin surface, and although surface mineral precipitation was inhibited, mineral ions entered the subsurface area [30, 31, 41]. Therefore, F entered the subsurface area even when it was covered with OPN. However, the percentage of remineralization was significantly lower in the 2.7 μM OPN group than in the control group, which was similar to that in the 5.4 μM OPN group. The reasons for these results currently remain unknown, which is a limitation of the present study. One possibility is that needle-like structures at the surface precipitation of enamel supply minerals to subsurface areas.

Further studies are needed to elucidate the underlying mechanisms.

The application of protein to the enamel surface at a high concentration has been shown to inhibit enamel remineralization [41]. We measured the concentration of OPN based on previous findings showing that 1.5 and 2.7 μM of bovine milk OPN effectively inhibited initial oral bacteria adhesion [27] and also reduced biofilm formation and pH drops in dental biofilms [26, 28, 42, 43]. We used 1 ppm of F, which was previously reported to be effective for dental caries prevention [30, 41]. Our results showed 2.7 μM OPN inhibited remineralization whereas 5.4 μM OPN recovered remineralization in solution with F. The present results indicate that 5.4 μM of bovine milk OPN with 1 ppm of F solution would contribute to facilitate ion bioavailability for remineralization.

In conclusion, the remineralization of demineralized enamel was achieved despite the application of bovine milk OPN prior to immersion in solution with F. Although bovine milk OPN exerts a number of antibacterial effects on oral bacteria, it has not yet been applied to clinical settings. Therefore, application of 5.4 μM bovine milk OPN prior to immersion in solution with F would be a potential for the management of dental caries in the future, from a viewpoint of both bacteria and remineralization.

Declarations

Acknowledgments

We thank Professor Seikou Shintani (Department of Pediatric Dentistry, Tokyo Dental College) for his helpful suggestions.

Funding

The present study was supported in part by a grant from the Multidisciplinary Research Center for Jaw Disease (MRCJD) from Tokyo Dental College.

Ethics approval and Consent to Participate

Ethics approval

This article does not contain any studies with human participants or animals performed by any of the authors.

Informed consent

Informed consent is not required in this study.

Conflicts of Interest

The authors have explicitly stated that there are no conflicts of interest.

Author Contributions

HI, HH, HK and TM contributed to design this study. HI, KN and YM conducted the experiments. HI, HH and TM analyzed and interpreted the data. HI, HH and TM drafted and critically revised the manuscript. All authors gave final approval and agree to be accountable for all aspects of the work.

References

1. Sollböhrer O, May KP, Anders M (1995) Force microscopical investigation of human teeth in liquids. *Thin Solid Films* 264:176–183. [http://dx.doi.org/10.1016/0040-6090\(95\)05847-8](http://dx.doi.org/10.1016/0040-6090(95)05847-8)
2. Dorozhkin SV (1997) Surface reactions of apatite dissolution. *J Colloid Interface Sci* 191:489–497. <http://dx.doi.org/10.1006/jcis.1997.4942>
3. Chen H, Tang Z, Liu J, Sun K, Chang SR, Peters MC, et al (2006) Acellular synthesis of a human enamel-like microstructure. *Adv Mater* 18:1846–1851. <http://dx.doi.org/10.1002/adma.200502401>
4. Arends J, Christoffersen J (1986) The nature of early caries lesions in enamel. *J Dent Res* 65:2–11. <http://doi.org/10.1177/00220345860650010201>
5. ten Cate JM (1999) Current concepts on the theories of the mechanism of action of fluoride. *Acta Odontol Scand* 57:325–329. <http://doi.org/10.1080/000163599428562>
6. Cochrane NJ, Cai F, Huq NL, Burrow MF, Reynolds EC (2010) New approaches to enhanced remineralization of tooth enamel. *J Dent Res* 89:1187–1197. <http://dx.doi.org/10.1177/0022034510376046>
7. Kidd EA, Fejerskov O (2016) *Essentials of Dental Caries*. Oxford University Press: UK; pp. 110–112. <http://dx.doi.org/10.1093/oso/9780198738268.001.0001>
8. Philip N (2019) State of the art enamel remineralization systems: the next frontier in caries management. *Caries Res* 53:284–295. <http://dx.doi.org/10.1159/000493031>
9. Milly H, Festy F, Watson TF, Thompson I, Banerjee A (2014) Enamel white spot lesions can remineralise using bio-active glass and polyacrylic acid-modified bio-active glass powders. *J Dent* 42:158–166. <http://dx.doi.org/10.1159/000493031>
10. Shen P, Walker GD, Yuan Y, Reynolds C, Stanton DP, Fernando JR, et al (2018) Importance of bioavailable calcium in fluoride dentifrices for enamel remineralization. *J Dent* 78:59–64. <http://dx.doi.org/10.1016/j.jdent.2018.08.005>
11. Karlinsey RL, Pfarrer AM (2012) Fluoride plus functionalized β -TCP: a promising combination for robust remineralization. *Adv Dent Res* 24:48–52. <http://dx.doi.org/10.1177/0022034512449463>
12. Pandya M, Diekwisch TGH (2019) Enamel biomimetics – fiction or future of dentistry. *Int J Oral Sci* 11:8. <http://dx.doi.org/10.1038/s41368-018-0038-6>
13. Denhardt DT, Guo X (1993) Osteopontin: a protein with diverse functions. *FASEB J* 7:1475–1482. <http://dx.doi.org/10.1096/fasebj.7.15.8262332>
14. Brown LF, Papadopoulos-Sergiou A, Berse B, Manseau EJ, Tognazzi K, Perruzzi CA, et al (1994) Osteopontin expression and distribution in human carcinomas. *Am J Pathol* 145:610–623.

15. Rittling SR, Novick KE (1997) Osteopontin expression in mammary gland development and tumorigenesis. *Cell Growth Differ* 8:1061–1069.
16. Fisher JL, Schmitt JF, Howard ML, Mackie PS, Choong PF, Risbridger GP (2002) An in vivo model of prostate carcinoma growth and invasion in bone. *Cell Tissue Res* 307:337–345.
<http://dx.doi.org/10.1007/s00441-001-0503-x>
17. Ohtsuka W, Ohta K, Isshiki Y, Kizaki H (2000) Quantitative analysis of osteopontin gene expression using a real time reverse transcription-polymerase chain reaction assay. *J Hard Tissue Biol* 9:47–55.
18. Muramatsu T, Ohta K, Asaka M, Kizaki H, Shimono M (2002) Expression and distribution of osteopontin and matrix metalloproteinase (MMP)-3 and – 7 in mouse salivary glands. *Eur J Morphol* 40:209–12. <http://dx.doi.org/10.1076/ejom.40.4.209.16689>
19. Asaka M, Ohta K, Muramatsu T, Kurokawa M, Kizaki K, Hashimoto S, et al (2006) The expression and localization of osteopontin in the mouse major salivary glands. *Arch Histol Cytol* 69:181–188.
<http://dx.doi.org/10.1679/aohc.69.181>
20. Holt C, Lenton S, Nylander T, Sørensen ES, Teixeira SC (2014) Mineralisation of soft and hard tissues and the stability of biofluids. *J Struct Biol* 185:383–396. <http://dx.doi.org/10.1016/j.jsb.2013.11.009>
21. Jiang R, Lønnerdal B (2016) Biological roles of milk osteopontin. *Curr Opin Clin Nutr Metab Care* 19:214–219. <http://dx.doi.org/10.1097/MCO.0000000000000275>
22. Nagatomo T, Ohga S, Takada H, Nomura A, Hikino S, Imura M, et al (2004) Microarray analysis of human milk cells: persistent high expression of osteopontin during the lactation period. *Clin Exp Immunol* 138:47–53. <http://dx.doi.org/10.1111/j.1365-2249.2004.02549.x>
23. Schack L, Lange A, Kelsen J, Agnholt J, Christensen B, Petersen TE, et al (2009) Considerable variation in the concentration of osteopontin in human milk, bovine milk, and infant formulas. *J Dairy Sci* 92:5378–5385. <http://dx.doi.org/10.3168/jds.2009-2360>
24. Christensen B, Sørensen ES (2016) Structure, function and nutritional potential of milk osteopontin. *Int Dairy J* 57:1–6. <http://dx.doi.org/10.1016/j.idairyj.2016.02.034>
25. Schack L, Stapulionis R, Christensen B, Kofod-Olsen E, Sørensen UBS, Vorup-Jensen T, et al (2009) Osteopontin enhances phagocytosis through a novel osteopontin receptor, the alpha X beta 2 integrin. *J Immunol* 182:6943–6950. <http://doi.org/10.4049/jimmunol.0900065>
26. Schlafer S, Raarup MK, Wejse PL, Nyvad B, Städler BM, Sutherland DS, et al (2012) Osteopontin reduces biofilm formation in a multi-species model of dental biofilm. *PLoS One* 7:e41534.
<http://dx.doi.org/10.1371/journal.pone.0041534>
27. Schlafer S, Meyer RL, Sutherland DS, Städler BM (2012) Effect of osteopontin on the initial adhesion of dental bacteria. *J Nat Prod* 75:2108–2112. <http://dx.doi.org/10.1021/np300514z>
28. Schlafer S, Ibsen CJ, Birkedal H, Nyvad B (2017) Calcium-Phosphate-Osteopontin Particles Reduce Biofilm Formation and pH Drops in in situ Grown Dental Biofilms. *Caries Res* 51:26–33.
<http://dx.doi.org/10.1159/000451064>
29. Kumura H, Minato N, Shimazaki K (2006) Inhibitory activity of bovine milk osteopontin and its fragments on the formation of calcium phosphate precipitates. *J Dairy Res* 73:449–453.

- <http://dx.doi.org/10.1017/S0022029906001877>
30. Romero MJ, Nakashima S, Nikaido T, Sadr A, Tagami J (2016) In vitro dentine remineralization with a potential salivary phosphoprotein homologue. *Arch Oral Biol* 68:35–42.
<http://dx.doi.org/10.1016/j.archoralbio.2016.03.014>
 31. Nakamura K, Hamba H, Miyayoshi Y, Ishizuka H, Muramatsu T (2021) *In vitro* remineralization of enamel with a solution containing casein and fluoride. *Dent Mater J* 40:1109–1114.
<http://dx.doi.org/10.4012/dmj.2020-383>
 32. Margolis HC, Zhang YP, Lee CY, Kent RL Jr., Moreno EC (1999) Kinetics of enamel demineralization *in vitro*. *J Dent Res* 78:1326–1335. <http://dx.doi.org/10.1177/00220345990780070701>
 33. ten Cate JM, Duijsters PP (1982) Alternating demineralization and remineralization of artificial enamel lesion. *Caries Res* 16:201–210. <http://dx.doi.org/10.1159/000260599>
 34. Neves Ade A, Countinho E, Vivian Cardoso M, Jaecques SV, Van Meerbeek B (2010) Micro-CT based quantitative evaluation of caries excavation. *Dent Mater* 26:579–588.
<http://dx.doi.org/10.1016/j.dental.2010.01.012>
 35. Jennings RJ (1988) A method for comparing beam-hardening filter materials for diagnostic radiology. *Med Phys* 15:588–599. <http://dx.doi.org/10.1118/1.596210>
 36. Hamba H, Nikaido T, Sadr A, Nakashima S, Tagami J (2012) Enamel lesion parameter correlations between polychromatic micro-CT and TMR. *J Dent Res* 91:586–591.
<http://dx.doi.org/10.1177/0022034512444127>
 37. Raj PA, Johnsson MJ, Levine MJ, Nancollas GH (1992) Salivary statherin. Dependence on sequence, charge, hydrogen bonding potency, and helical conformation for adsorption to hydroxyapatite and inhibition of mineralization. *J Biol Chem* 267:5968–5976. [http://dx.doi.org/10.1016/S0021-9258\(18\)42650-6](http://dx.doi.org/10.1016/S0021-9258(18)42650-6)
 38. Fedarko NS, Jain A, Karadag A, Fisher LW (2004) Three small integrin binding ligand N-linked glycoproteins (SIBLINGs) bind and activate specific matrix metalloproteinases. *FASEB J* 18:734–736. <http://dx.doi.org/10.1096/fj.03-0966fje>
 39. Ogbureke KU, Fisher LW (2004) Expression of SIBLINGs and their partner MMPs in salivary glands. *J Dent Res* 83:664–670. <http://dx.doi.org/10.1177/154405910408300902>
 40. Klänning E, Christensen B, Sørensen ES, Vorup-Jensen T, Jensen JK (2014) Osteopontin binds multiple calcium ions with high affinity and independently of phosphorylation status. *Bone* 66:90–95.
<http://dx.doi.org/10.1016/j.bone.2014.05.020>
 41. Fujikawa H, Matsuyama K, Uchiyama A, Nakashima S, Ujiie T (2008) Influence of salivary macromolecules and fluoride on enamel lesion remineralization *in vitro*. *Caries Res* 42:37–45.
<http://dx.doi.org/10.1159/000111748>
 42. Schlafer S, Birkedal H, Olsen J, Skovgaard J, Sutherland DS, Wejse PL, et al (2016) Calcium-phosphate-osteopontin particles for caries control. *Biofouling* 32:349–357.
<http://dx.doi.org/10.1080/08927014.2016.1141199>

43. Kristensen MF, Zeng G, Neu TR, Meyer RL, Baelum V, Schlafer S (2017) Osteopontin adsorption to Gram-positive cells reduces adhesion forces and attachment to surfaces under flow. *J Oral Microbiol* 9:1379826. <http://dx.doi.org/10.1080/20002297.2017.1379826>

Tables

Table 1: Mean percentage of remineralization for each experimental group. Data were expressed as mean (%) \pm standard deviation (SD). The percentage of remineralization was higher in the F (+) group than in the F (-) group in the control, OPN 2.7 μ M, and OPN 5.4 μ M groups at 7 and 14 days. The same capital letters in 7d and 14d are not significantly different ($p > 0.05$). The same small letters in each group are not significantly different ($p > 0.05$).

7d: after 7 days of remineralization; 14d: after 14 days of remineralization; OPN: osteopontin;

n = 9 per group; F: remineralizing solution containing F (1 ppm).

Mean percentage of remineralization (%R)

	7 d	14 d
Control	24.27 \pm 3.84 ^{Aa}	41.90 \pm 2.84 ^{Bd}
F, Control	42.29 \pm 2.81 ^{Ab}	51.40 \pm 2.97 ^{Bf}
OPN 2.7 μ M	20.70 \pm 4.89 ^{Aa}	36.91 \pm 2.84 ^{Be}
F, OPN 2.7 μ M	36.22 \pm 4.10 ^{Ac}	42.53 \pm 3.59 ^{Bd}
OPN 5.4 μ M	20.17 \pm 3.68 ^{Aa}	33.87 \pm 2.78 ^{Be}
F, OPN 5.4 μ M	37.38 \pm 2.08 ^{Abc}	47.39 \pm 4.04 ^{Bf}

(n = 9 each)

Figures

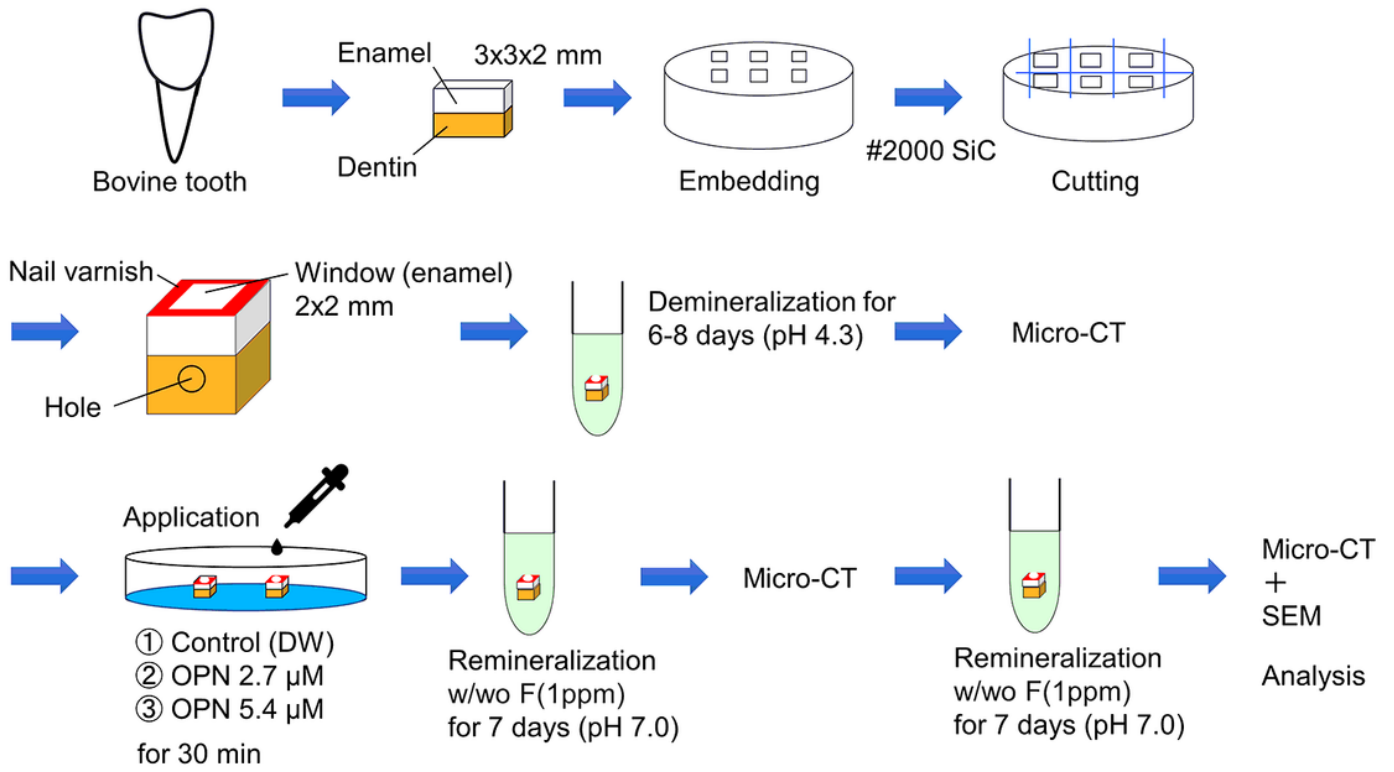


Figure 1

Schematic representation of specimen preparation and scanning by micro-CT and SEM.

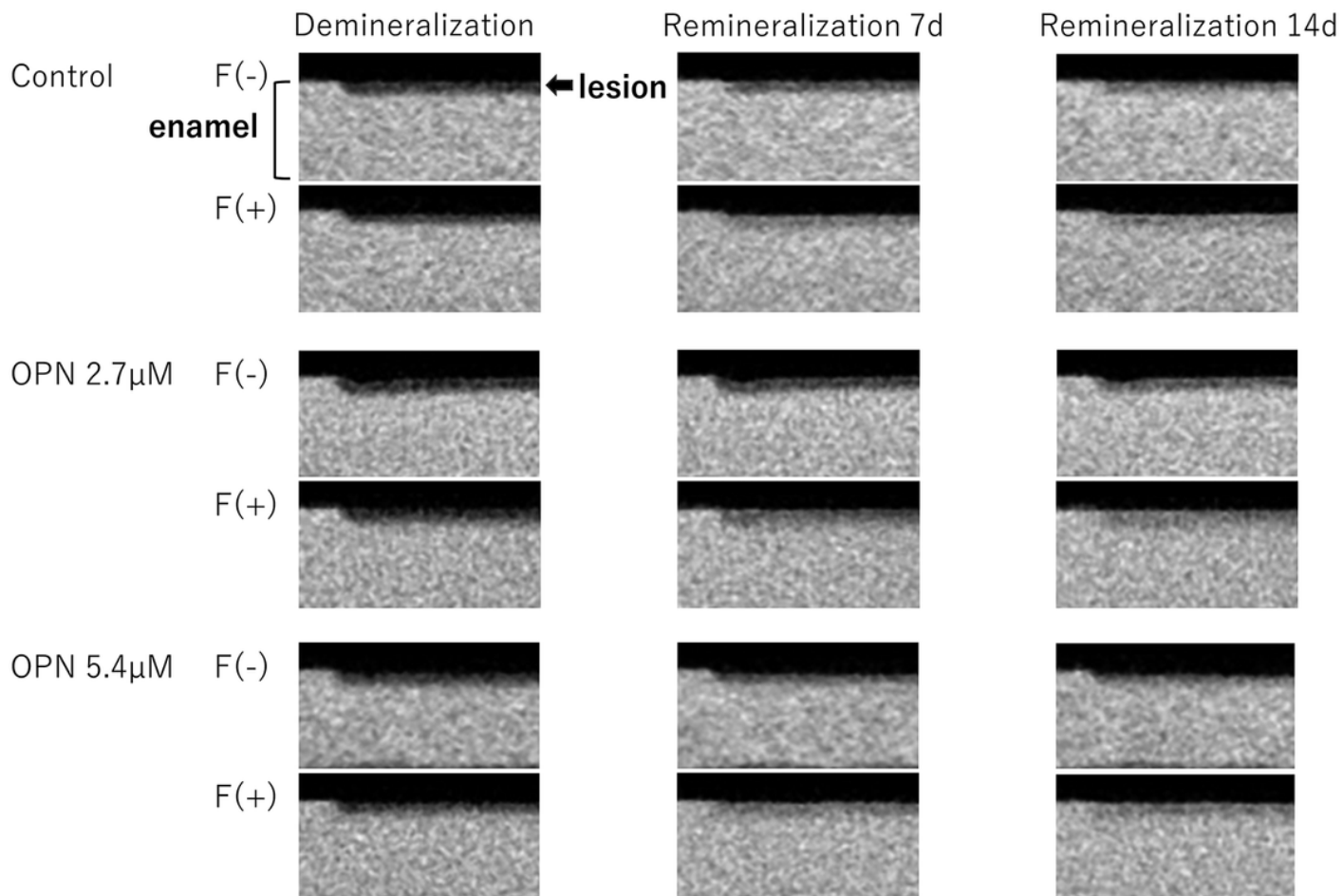


Figure 2

2D micro-CT images of single specimens from each group. 2D images of the control, OPN 2.7 μM, and OPN 5.4 μM groups are shown after demineralization and after 7 and 14 days of remineralization. After demineralization, an X-ray transmission image was obtained showing lesions on the surface layer of enamel. After 7 and 14 days of remineralization, the radiopacity of the areas was increased in all groups.

7d: after 7 days of remineralization; 14d: after 14 days of remineralization; OPN: osteopontin;

F: remineralizing solution containing F (1 ppm).

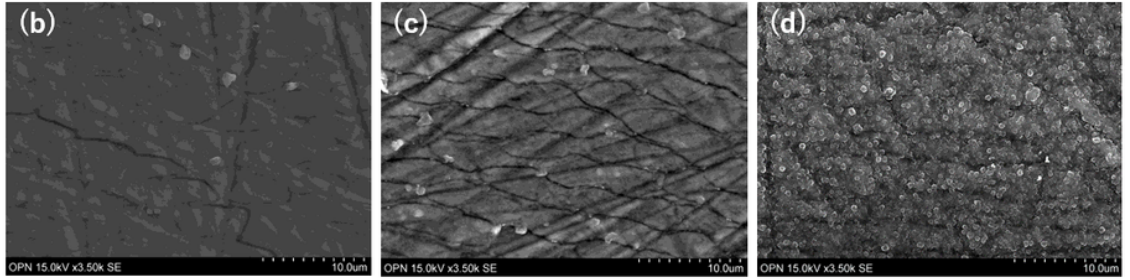
Surfaces

Remineralization 14d

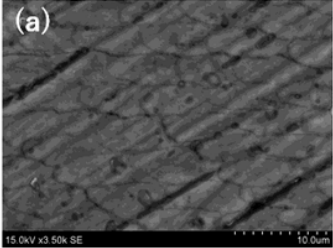
Control
F(-)

OPN 2.7 μ M

OPN 5.4 μ M



Demineralization



F(+)

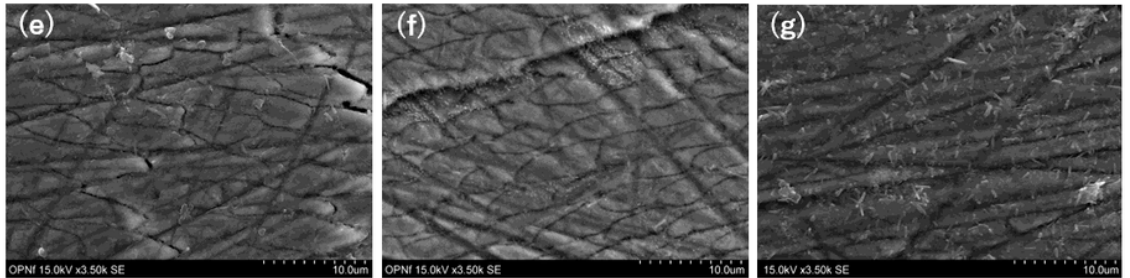


Figure 3

SEM micrographs of enamel surfaces in the control group after demineralization (a), and in control (b, e), OPN 2.7 μ M (c, f) and OPN 5.4 μ M (d, g) groups after 14 days of remineralization. After remineralization, crystal-like deposits were observed (c, d) in the F (-) group. Needle-like deposits were noted in the F (+) group (e to g).

14d: after 14 days of remineralization; OPN: osteopontin;

F: remineralizing solution containing F (1 ppm).

Cross-sectional

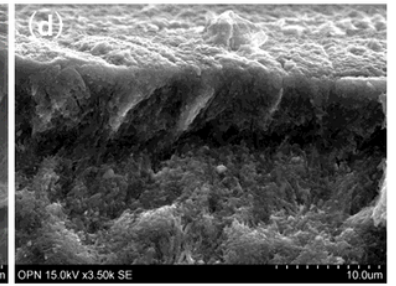
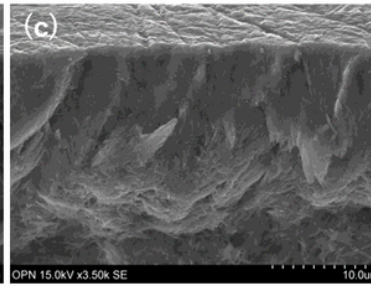
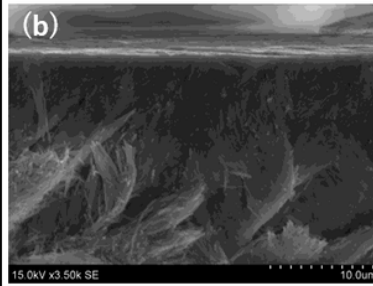
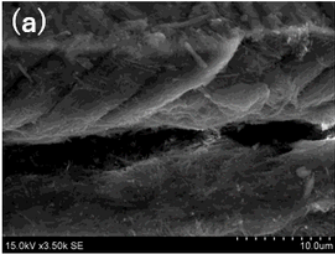
Remineralization 14d

Control
F(-)

OPN 2.7 μ M

OPN 5.4 μ M

Demineralization



F(+)

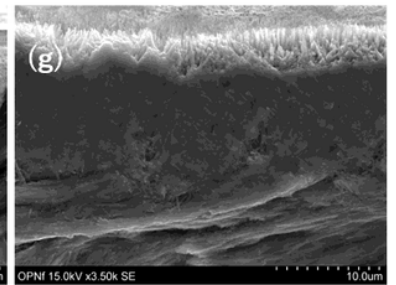
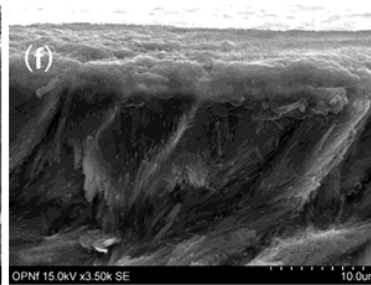
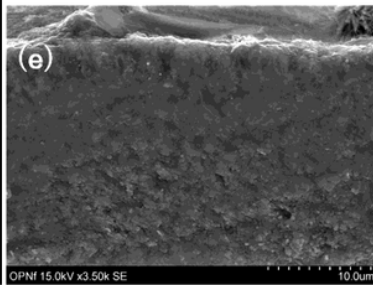


Figure 4

Cross-sectional SEM micrographs of enamel specimens in the control group after demineralization (a) and in control (b, e), OPN 2.7 μ M (c, f), and OPN 5.4 μ M (d, g) groups after 14 days of remineralization. After demineralization, a sparse structure was confirmed at the subsurface region (a). In the F (-) group, the sparse structure disappeared in the control group (b), but remained in the OPN (+) groups (c, d). In the F (+) group, the sparse structure disappeared compared with the F (-) groups (e to g).

14d: after 14 days of remineralization; OPN: osteopontin;

F: remineralizing solution containing F (1 ppm).